University of Baghdad
College of Engineering
JE
JOURNAL OF ENGINEERING

Journal of Engineering

journal homepage: www.joe.uobaghdad.edu.iq

Volume 30 Number 2 February 2024

Numerical Study of Composite Concrete Castellated Double Channel Beams with Strengthening Techniques

Nihad Yaseen Abbas[1,*], Ahmad Jabbar Hussain Alshimmeri[2]

Department of Civil Engineering, College of Engineering, University of Baghdad, Baghdad, Iraq
nihad.y.abbas1901p@coeng.uobaghdad.edu.iq[1], dr.ahmadalshimmeri@coeng.uobaghdad.edu.iq[2]

ABSTRACT

Current numerical research was devoted to investigating the effect of castellated steel beams without and with strengthening. The composite concrete asymmetrical double hot rolled steel channels bolted back to back to obtain a built-up I-shape form are used in this study. The top half part of the steel is smaller than the bottom half part, and the two parts were connected by bolting and welding. The ABAQUS/2019 program employed the same length and conditions of loading for four models: The first model is the reference without castellated and strengthening; the second model was castellated without strengthened; the third model was castellated and strengthened with reactive powder concrete encased in the steel web, and the fourth model was castellated and strengthened with reactive powder concrete and lacing steel rebar's welded diagonally on two sides of the steel web. According to the Numerical results, there was an increase in ultimate load capacity compared to the reference model of about 22.74%, 51.65%, and 77.98% in the second, third, and fourth models, respectively; also, there is a reduction in deflection of 55.52%, 58.74, and 60.55% in the second, third, and fourth models, respectively, compared to the level deflection at ultimate load for the reference model, with an increase in stiffness and ductility. In comparison to the I section, the fabrication of a castellated steel beam from the double channel is more cost-effective in terms of cutting steel loss at the ends of the castellated beam, this is due to the feature of rotation and reflection of the steel channel section during cutting and forming to castellated shape.

Keywords: Composite beams, Double steel channel, Castellated beams, Finite element analysis, Strengthening, Flexure.

*Corresponding author
Peer review under the responsibility of University of Baghdad.
https://doi.org/10.31026/j.eng.2024.02.03

Article received: 22/08/2023
Article accepted: 21/10/2023
Article published: 01/02/2024

الدراسة العددية للعتبات المركبه من الخرسانه وقلعوية حديد الساقية المزدوج مع تقنيات التقوية

نهاد ياسين عباس*، احمد جبار حسين الشمري

قسم الهندسة المدنية، كلية الهندسة، جامعة بغداد، بغداد، العراق

الخلاصة

تم تخصيص البحث العددي (النظري) الحالي لدراسة تاثير استخدام العتبات الفولاذية ذات الفتحات القلعوية بدون التقوية ومع التقوية العتبة المركبة من الخرسانة ومزدوج حديد الساقية الغير متناظر المربوط بالبراغي من جهه الظهر لتشكيل مقطع يشبه الحرف (I) باللغه الانجليزيه قد استخدم في هذه الدراسة . نصف الجزء الاعلى اكبر من نصف الجزء الاسفل بالنسبة لمقطع الحديد والاجزاء العلوية والسفلية ربطت عن طريق البراغي واللحام الكهربائي استخدم برنامج ABAQUS / 2019 لتحليل جميع العتبات بنفس الطول وحاله التحميل لأربعة نماذج: النموذج الأول هو المرجع بدون التشكيل على القلعوية وبدون التقوية، النموذج الثاني كان فيه التشكيل على القلعوية وبدون استخدام التقوية النموذج الثالث فيه التشكيل على القلعوية مع تقوية بمسحوق الخرسانة الفعالة التي بها تم اكساء الجذع الفولاذي من الجهتين والنموذج الرابع استخدم التشكيل القلعوي للحديد مع التقوية بمسحوق الخرسانة الفعالة وقضبان التسليح الملامسة والملحومة بشكل مائل على جانبي الجذع الفولاذي للعتبة. وفقا الى نتائج التحليل العددي فان هناك زياده بسعه التحميل الاقصى مقارنة بتحمل النموذج المرجعي بحوالي 22.74٪ و 51.65٪ و 77.98٪ في النماذج الثاني والثالث والرابع على التوالي ؛ أيضًا ، هناك انخفاض في الهطول بنسبة 55.52٪ و 58.74 و 60.55٪ في النماذج الثاني والثالث والرابع ، على التوالي مقارنةً بمستوى الهطول عند الحمل النهائي للنموذج المرجعي ، مع زيادة الصلابة والمطيلية. بالمقارنة مع التشكيل القلعوي لمقطع (I) ، فإن تصنيع العوارض الفولاذية القلعوية من قناة مزدوجة يكون أكثر فعالية واقتصاديا بالنسبة الى خسارة قطع الفولاذ في نهايات العتبة القلعوية و ذلك يرجع إلى خاصية الدوران والانعكاس لمقطع القناة الفولاذية أثناء القطع والتشكيل القلعوي.

الكلمات المفتاحية :العتبات المركبة،ساقية حديد مزدوجة،العتبات القلعويه،تحليل العناصر المحدده،التقوية ، الانثناء.

1. INTRODUCTION

Castellated steel beams with extended parts with hexagonal perforations, as well as castellated steel beams with hexagonal apertures, were largely employed. The Chicago Bridge and Iron Works was the primary user of Castellated steel beams in 1910 **(Das, 1984)**. G.M. was also personally involved in this **(Boyed, 1964)** and also subsequently adopted in the United Kingdom **(Knowles and BS 5950, 1991). (Altifillisch et al., 1957; Toprac and Cooke, 1959)** explained the Vierendeel failure kind for the failure mode of the castellated steel beam. This occurred by a big shear load applied to the beam. The plastic hinges at the portholes corner distort the tee section top and bottom holes in the fourth edges.

As a result of researchers' efforts to create new processes to enhance the construction and structural performance of building parts, castellated beams are one of the most recent innovations to be relied upon in constructing structures **(Fares et al., 2016)**. **(Waryosh and Ali, 2020)** investigated the behaviour of the polymer concrete composite castellated beam using geopolymer concrete that was cast above the castellated steel beam with different

opening shapes, test results showed that the hexagon opening shape gave more strength capacity and less deflection and slip. Also, the full interaction gave more strength capacity and less deflection and slip. The decrease in slip in case of full interaction than partial is 34.13 and 82.08% for the hexagon and rectangular openings, respectively.

(Khaleel and AL-Shamaa, 2021) Investigated the structural performance of double channel steel beams bolted back to back to form a built-up I-shaped form. Five specimens of different sections were tested with the same length and all testing parameters conditions, with only a difference in the number of openings. The study showed that when the web holes are few, the total bearing strength decreases. When the number of web holes increased to a specific limit, the rate of development in the bearing force was determined to be between 17.7% and 40.0% and when openings exceeded a specific limit, the bearing force decreased. Reactive Powder Concrete (R.P.C.) is a cementation material that is added to reinforced concrete mixes or used as an overlay to improve the mechanical and chemical qualities of the member that was placed on it **(Qasim, 2019)**.

The results presented by **(Hadeed and Alshimmeri, 2019)** show that the load-carrying capacities of the three castellated steel beams with different configurations: without strengthening, strengthening with only R.P.C., and using R.P.C. reinforced with rebar lacing were raised by 39.11%, 105.95%, and 124.77%, respectively, when compared to the origin solid beam. Show that the load-carrying capacities of the three castellated steel beams with different configurations: without strengthening, strengthening with only R.P.C., and using R.P.C. reinforced with rebar lacing were increased by 39.11%, 105.95%, and 124.77%, respectively, when compared to the origin solid beam **(Ammar and Alshimmeri, 2021).** The load-carrying capacity of asymmetrical castellated beams with encasement by R.P.C. with lacing reinforcement at the steel web was experimentally studied; the tested results show a decrease in deflection of approximately 33.33, 52.77, and 27.78%, respectively, with an increase in ultimate load capacity of about 26.92, 46.15, and 9.23%, respectively, compared with the reference specimen. Under harmonic load, lightweight concrete deck slabs behave similarly to normal-weight concrete deck slabs. When fibres were added to the mix, the results showed a significant improvement in cracking load, ultimate load, concrete toughness index, and ductility, indicating that adding fibres is a good choice for normal-weight concrete deck slabs **(Dakhel and Mohammed, 2022).**

(Al-Tameemi and Alshimmeri, 2023) investigated the theoretical behaviour of an asymmetrical composite concrete castellated steel beam with encased steel web by R.P.C. with laced rebar as a strengthening effect by employing a gap (no welding) between two halves of steel web. The researchers presented and analysed four specimens of the same length (3m) subjected to two-point static loadings with simply supported reactions, resulting in increased ultimate load by using gaps (10% and 20%) from the total original steel depth equal to (3.39% and 11.25%), respectively, and decrease by (19.87%) with a gap equal to zero. (**Mohammed and Ali, 2023**) used Concrete Damage Plasticity (CDP) to the concrete model, and the steel is modelled as elastic perfectly plastic, while R.P.C. with steel fibre applied stress-strain relation suggested by (**Collins et al., 1993). (Al-Hilali and Izzet, 2023)** created a numerical nonlinear FEA damage plasticity model to replicate current non-prismatic prestressed concrete beams with varied multi-opening configurations. The tested specimens were numerically validated until a satisfactory degree of precision was achieved using a good FEA modeling technique and completely exact material modes.

The current numerical study of the effect of castellation without or with strengthening by R.P.C., and lacing steel rebars (welded diagonally on two sides of the steel web) on the

flexural behaviour of a composite concrete solid asymmetrical double hot rolled steel channel beam, using the same properties of the material and conditions of loading.

2. MATERIALS AND METHODS

2.1 Fabricating and Details of Models

All four composite beam models were designed in the same dimensions of concrete deck slab (3300×450×70) mm with mesh reinforcement and deformed steel bars (Ø8mm) with a spacing of (100mm) c/c in both ways. The Steel Beam (S.B.) in model No.1 consists of an asymmetrical double steel channel, the top half steel part made from the (2C7×12.25) section, and the bottom half steel part made from the (2C813.75) section; the two parts were connected by welding and connected back-to-back by bolts. The castellated Beam (C.B.) in model No.2 is the same as it begins by taking each channel and using Computer Numerical Control CNC to cut limiting zigzag lines with a cutting angel (45º) along the channel's web as two asymmetrical halves. Next, both parts are separated by sides to make four parts from two channels. Next, it was reconnected by welding on web posts for two selected parts to create two castellated channels with new opening patterns; finally, two castellated channels were connected back to back by bolts to produce the C.B. with an increase in the depth of about 1.5 times compared with the original steel beam in model No.1, before the castellated process **(Knowles and BS 5950, 1991).** It is worth noting that steel channels are characterised by the freedom of rotation and reflection when cutting to castellated form without losses in cutting steel at the edges of the castellated beam, unlike what is found in the castellated I section", see **Table 1** and **Fig.1**.

Table 1. The details of double channel sections **(AISC-2017).**

Channel Shape	G	d	b_f	t_w	t_f	r_x	A	I_x
2C7×12.25	36.42	177.8	111.24	15.8	9.29	65.4	4632	$20.07*10^6$
2C8×13.75	40.88	203.2	118.8	15.8	9.9	75.9	5200	$30*10^6$

G is the weight of the section, (kg/m), d is the depth of the section (mm), b_f is the width of the flange (mm), t_w is the web thickness (mm), r_x is the root radius(mm), t_f is the flange thickness (mm), A is the section area (mm^2), I_x is the moment of inertia about the x-axis (mm^4).

The C.B. model No.3 strengthened with R.P.C. (30 mm) with each side of steel web, while, the C.B. model No.4 strengthened with R.P.C.and lacing steel rebars (Ø6mm welded diagonally angel (45º) on two sides of the steel web), see **Fig. 2** and **Table 2.** Also, all models have the same length and boundary condition supported with two concentrated static loads. **Fig. 3** illustrates all details and measurements of all analysis models.

Table 2. Steel castellated details of models.

Model No.	dg	e	dt_{top}	dt_{bot}	$\theta°$	S	h_o
1	260.4	-	-	-	-	-	-
2, 3, 4	360.4	100	38.9	51.5	45	400	200

dg is the depth of the expanded beam (mm), e is the Distance between holes (mm), dt_{top} is the depth of the top tee(mm), dt_{bot} is the depth of the bottom(mm), $\theta°$is the Angle of cutting(degree), S is the Center-to-center distance between openings (mm), h_o is the Height of openings of the castellated beam (mm),

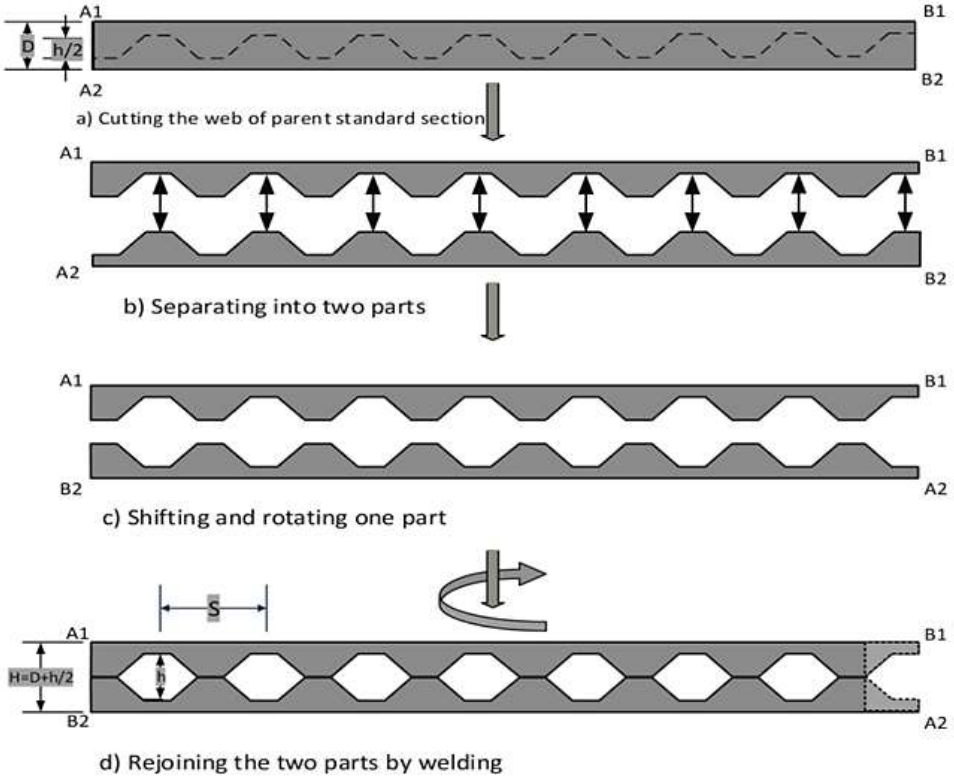

Figure 1. The manufacturing method of the castellated steel beam **(Al-Thabhawee, 2017).**

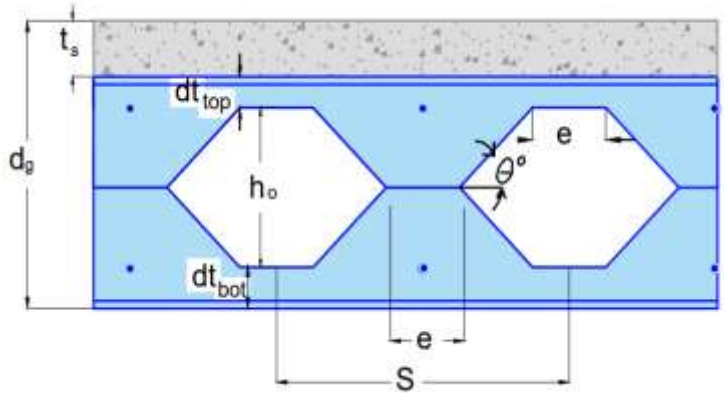

Figure 2. Denoted dimensions of castellated models.

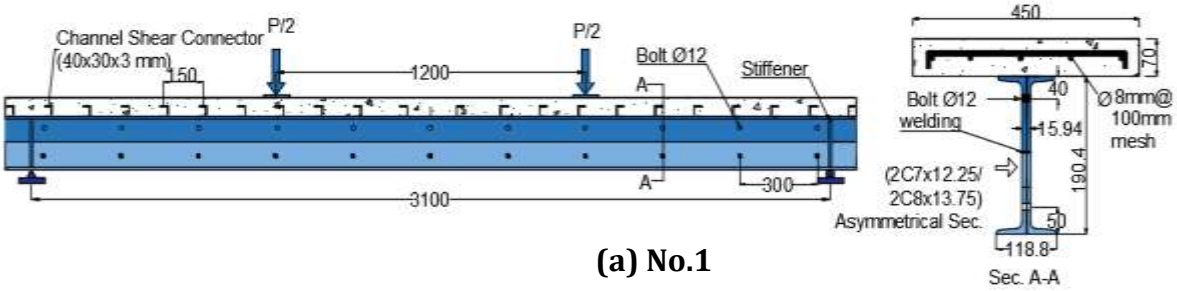

(a) No.1

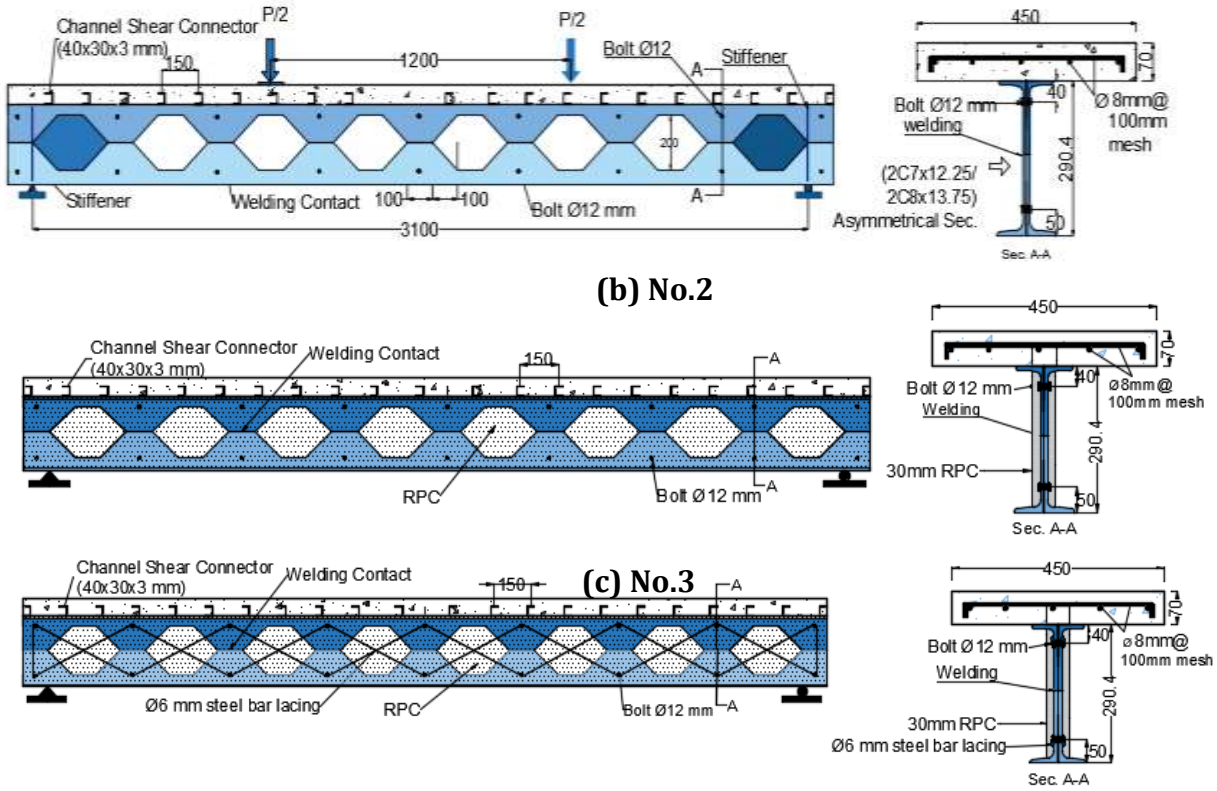

Figure 3. Models section details (all dimensions are in mm).

2.2 Material Characteristics

Mechanical properties of steel components, Normal Strength Concrete (N.S.C.) in deck slab and R.P.C. are illustrated in **Tables 3 and 4**, were adopted in this numerical study.

Table 3. Mechanical characteristics of the steel.

Steel sample	Thickness (mm)	Yield stress (f_y) (MPa)	Ultimate stress (fu) (MPa)
C7×12.25 (Web) (flange)	 7.9 9.2	 381 340	 574 585
C8×13.75 (Web) (flange)	 7.9 9.9	 390 396	 621 554
Stiffeners	12	390	621
Shear connectors Steel channel	3	456	615
Slab Reinforcement	(8 mm) diameter	420	623.5
Rebar Lacing	(6 mm) diameter	430	640

The hex bolts and nuts' mechanical properties have a diameter of 12mm, and fu are equal to 640 MPa and 800 MPa, respectively, according to **(BS 5950, 2000)**

Table 4. Mechanical properties of hardened slab concrete and R.P.C.

Conc. type	Model No.	f'_c	f'_{ct}	fr	E_c
N.S.C.	1,2,3,4	28.50	3.92	3.41	24250
R.P.C.	3,4	72.1	13.8	11.51	45500

f'_c is the concrete compressive strength (MPa). f'_{ct} is the concrete splitting tensile strength (MPa). f_r is the concrete modulus of rupture (Mpa). E_c is the modulus of elasticity of concrete (MPa)

3. RESULTS OF FINITE ELEMENT METHOD

3.1 Finite Element Modelling

The finite element method was used to provide approximate solutions for many intricate structural issues by splitting the structure into finite components or elements and then combining them in such a way as to illustrate the structure's deformations under the indicated load **(Matthews et al., 2000)**. For numerical modelling, the finite element program **(CAE Abaqus, 2019)** was utilized. To calculate the maximum deflection and ultimate load at mid-span for all investigated castellated beams subjected to a two-point load located upper two openings of a castellated beam, under the simple supported reactions, (Ux=Uy=Uz=0) was used to ensure the constraining of one of the supports and act as the hinge, while the y and z directions (Uy=Uz=0), to model a roller support.3.1.1 Concrete modeling

According to **(Oukaili and Al-Shammari, 2014)**, concrete is a quasi-brittle material that behaves differently in compression and tension. This material was modelled using the Solid65 element. This element has eight nodes, each with (3) degrees of freedom translation in the x, y, and z directions. This element can bend plastically, crack in three orthogonal directions, and crush. The self-weight of the beams was examined, and the Poisson's ratio (v) for concrete was assumed to be 0.2 **(Bangash, 1989)**. When a crack occurs, ABAQUS uses smeared cracks to execute constitutive calculations independently at each integration point of the finite element model, with the presence of cracks considered **(Abdullah, 1993)**. Tension stiffening can be modeled numerically by varying the stiffness of reinforcing bars or increasing the stiffness of concrete such that it can carry the tensile force following cracks **(Chaudhari and Chakrabarti, 2012)**.

(Hafezolghorani et al., 2017) studied the damage states in the compression and the tension which indicated by ε_c^{pl} and ε_t^{pl}, which referred to equivalent plastic strains in tension and compression, respectively. The plastic hardening strain in compression cpl played a crucial role in determining the relationship between the damage parameters and the compressive strength of concrete in the compressive behavior of ABAQUS program (CDP) models. as illustrated in **Fig. 4 (Lubliner et al., 1989)**.

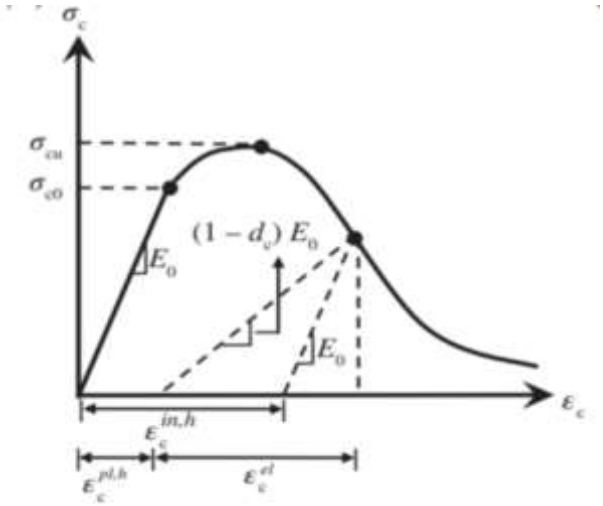

Figure 4. strain-stress diagram of concrete under compression uniaxial loading condition.

In return**,** the ABAQUS program will internally compute the plastic strain evaluated according to Eq. (1):

$$\boldsymbol{\varepsilon}_c^{\boldsymbol{pl},h}=\boldsymbol{\varepsilon}_c^{in,h}-[d_c\times\sigma_c/(1-d_c)E_0] \quad (1)$$

where; $\varepsilon^{in,c}$: inelastic compression strain, d_c: scalar compression damage variable, σ_c: nominal compressive stress and E_0: the initial Young's modulus.

(Reddiar, 2010) the strain is one-tenth that corresponding in compression (ε_{cu}). ε_{cu} is evaluated according to Eq. (2):

$$\varepsilon_{cu} = 0.012 - 0.0001f'(in\ MPa) \quad (2)$$

From **Fig. 5**, the plastic hardening strain in tension ε_t^{pl} was derived by Eq. (3):

$$\boldsymbol{\varepsilon}_t^{\boldsymbol{pl},h}=\boldsymbol{\varepsilon}_t^{ck,h}-[d_t\times\sigma_t/(1-d_t)E_0] \quad (3)$$

Where; ε^{ck}: tension strain, d_t: scalar tension damage variable, σ_t: nominal tension stress, E_0: modulus of elasticity.

(Alkloub et al. 2019) using an ultimate cracking strain of 0.00154, while the strain at failure calculated from the material properties is ($3.86/22960 = 1.68 \times 10-4$); it is 9.16-times $\varepsilon_{cr,failure}$. At any point, the cracking strain ε_{cr} is evaluated according to Eq. (4):

$$\varepsilon_{cr} = \varepsilon_t - (\sigma_t/E_o) \quad (4)$$

In the ABAQUS program the Concrete Damage Plasticity where flow parameters: Dilation angle= (30 to 40), Eccentricity=(0.1), (Fb_o/Fc_o)= (1.16), K=(2/3) and Viscosity parameter=(0.0001). (**Lee et al., 1998)**, see **Fig. 6**.

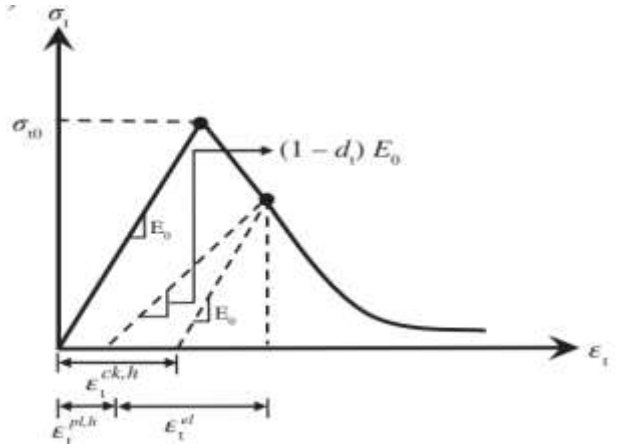

Figure 5. Strain-stress diagram of concrete under tension uniaxial loading condition **(Lubliner et al., 1989)**.

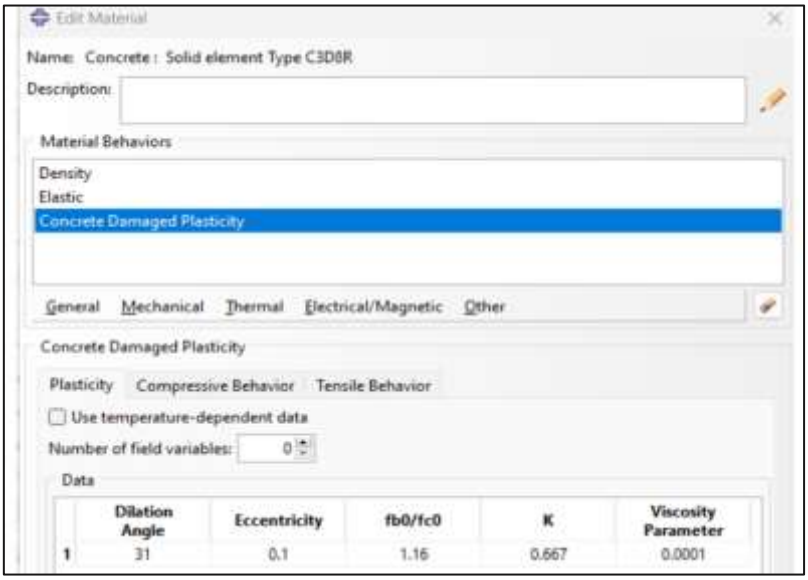

Figure 6. Parameters value of the Concrete Damage Plasticity in this study.

Dilation angle (ψ): This is the material's internal friction angle; in other words, the increase in plastic volume of concrete is more than the value of critical stress. As a result, the dilation angle had a significant impact on the overall model. The flexibility of the system was increased as the dilation angle was raised. However, greater values have been effectively used in recent study. For use with reinforced concrete, a value of =56o was chosen **(Demir et al., 2016)**.

3.1.1 Steel modelling

As for steel material, stress–strain relationship is linear elastic up to yielding, perfectly plastic between the yielding point and the beginning of strain hardening, as shown in **Fig. 7.** Since the analysis involves large inelastic strains, the nominal static stress–strain curves obtained from the coupons test were converted to true stress and logarithmic plastic true strain curves. The true stress ($\boldsymbol{\sigma_{true}}$) and plastic true strain ($\boldsymbol{\varepsilon}^{\boldsymbol{pl}}{}_{\boldsymbol{true}}$) were calculated using Eqs. (5) and (6), respectively.

$$\boldsymbol{\sigma_{true}} = (1 + \varepsilon) \qquad (5)$$

$$\boldsymbol{\varepsilon}^{\boldsymbol{pl}}{}_{\boldsymbol{true}} = \ln(1+\varepsilon) - (\sigma_{true}/E_0) \quad (6)$$

Where: E_0 is the initial Young's modulus, ($\boldsymbol{\sigma}$) and ($\boldsymbol{\varepsilon}$) are the measured nominal stress and strain values, respectively **(ABAQUS theory guide)**.

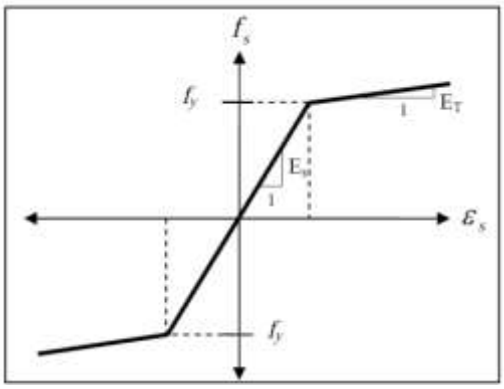

Figure 7. Bilinear stress–strain curves for steel **(ABAQUS User Guide, 2013).**

3.1.2 Finite element representation of composite concrete steel members

For the sake of this study's modelling, six parts were necessary. The first part was asymmetrical double-rolled steel channel shape sections to make the castellated steel beam (webs and flanges) as a solid element that is a continuum 3D 8-node hexahedral of type C3D8R as shown in **Fig.8**. The second part was the RPC filling the sides of the web as a solid element, that is, quadratic tetrahedral elements of type C3D10 as shown in **Fig.9**, while its reinforcement, the rebar lacing, was simulated using an element of type C3D8R, also The third part was a deck slab as a solid element of type C3D8R as shown in **Fig.10**, and its reinforcement bars were simulated using an element of type T3D2. The fourth part was a stiffener plate (at supports) as an element of type C3D8R. Also, the fifth part was a stiffener plate (at supports) as a solid element of type C3D8R. Finally, the sixth part the small steel channel as a shear connecter was simulated using quadrilateral elements of type S4R. These elements proved sufficient **(Ellobody, 2014)**; they were used to imitate the strong contact and friction between the web channel and the laced reinforcement. Both material geometry and nonlinearity were taken into account by the finite element models, the modelling shape in a finite element for models all as shown in **Fig. 11.**

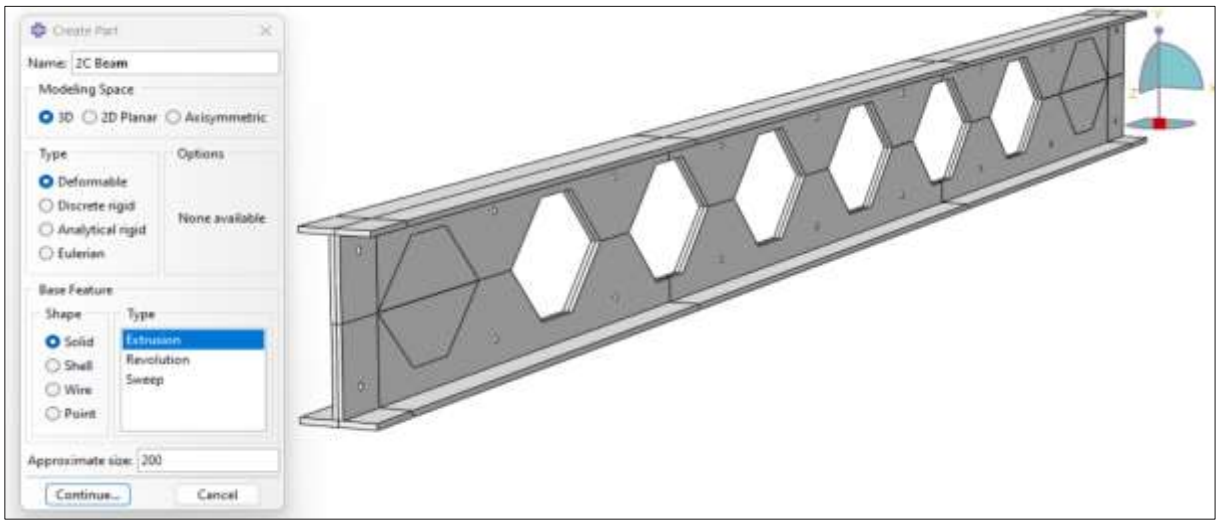

Figure 8. Modeling of the double steel channel section (webs and flanges) as parts.

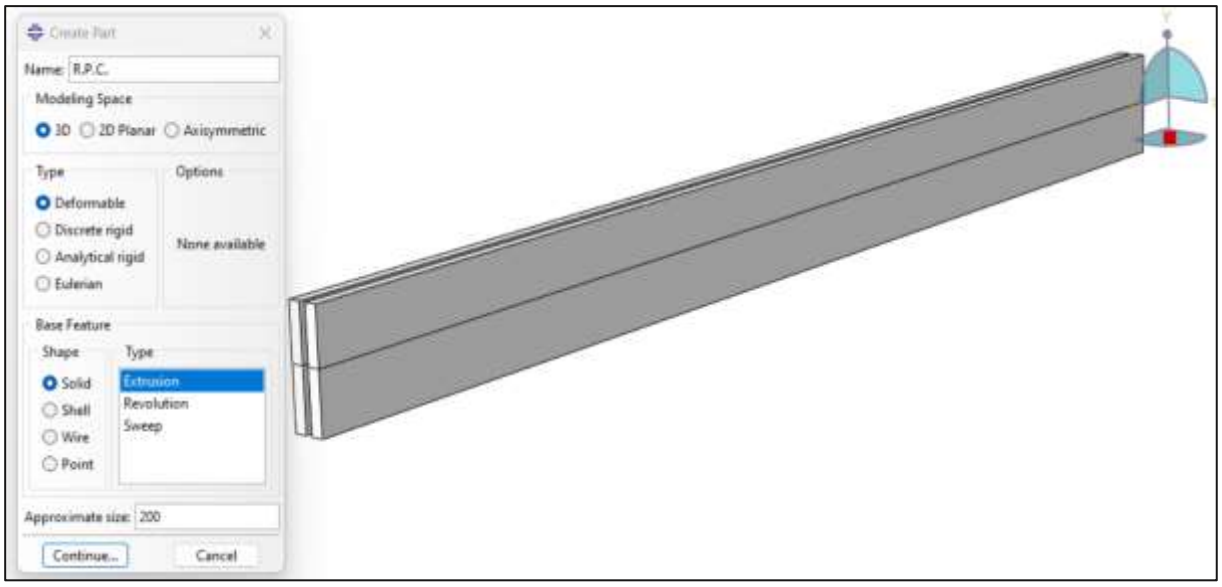

Figure 9. Modeling of reactive powder concrete as solid elements.

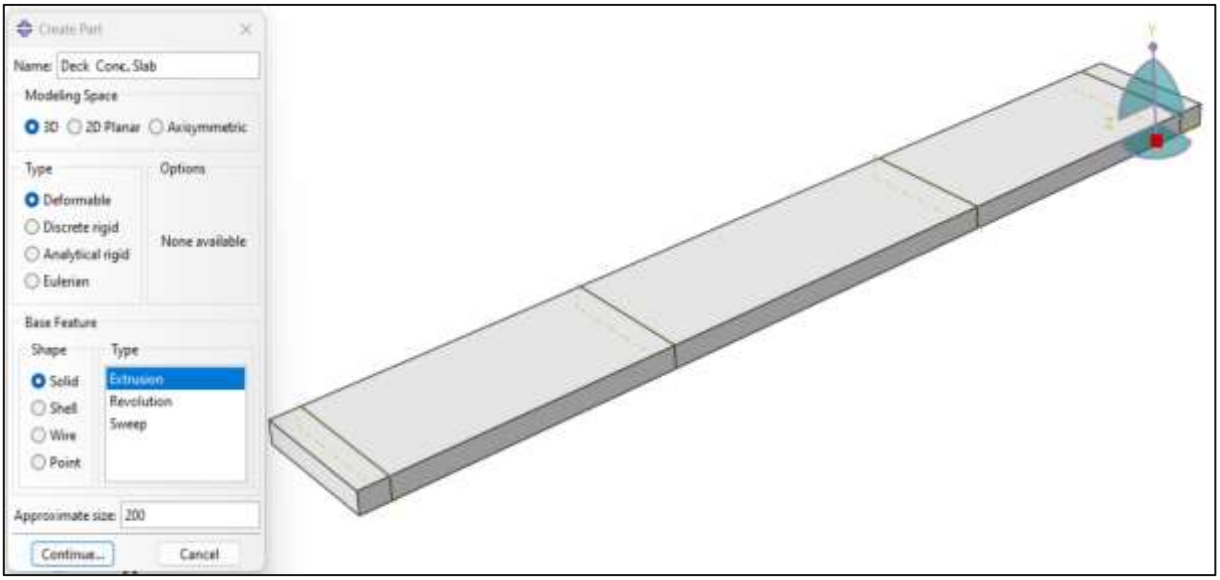

Figure 10. Modelling of the concrete slab.

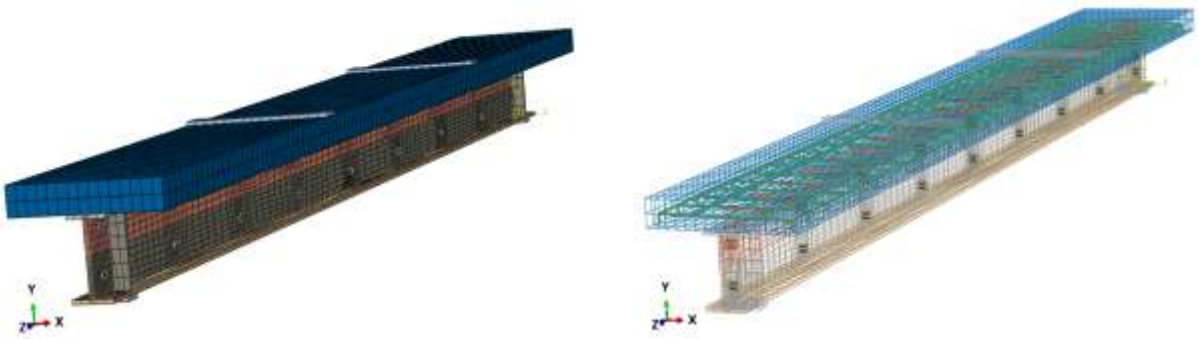

(a) No.1

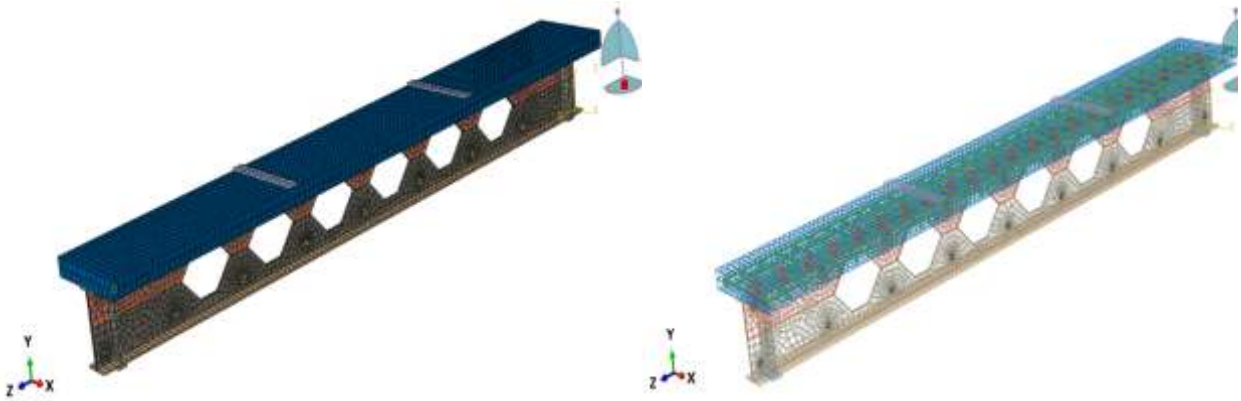

(b) No.2

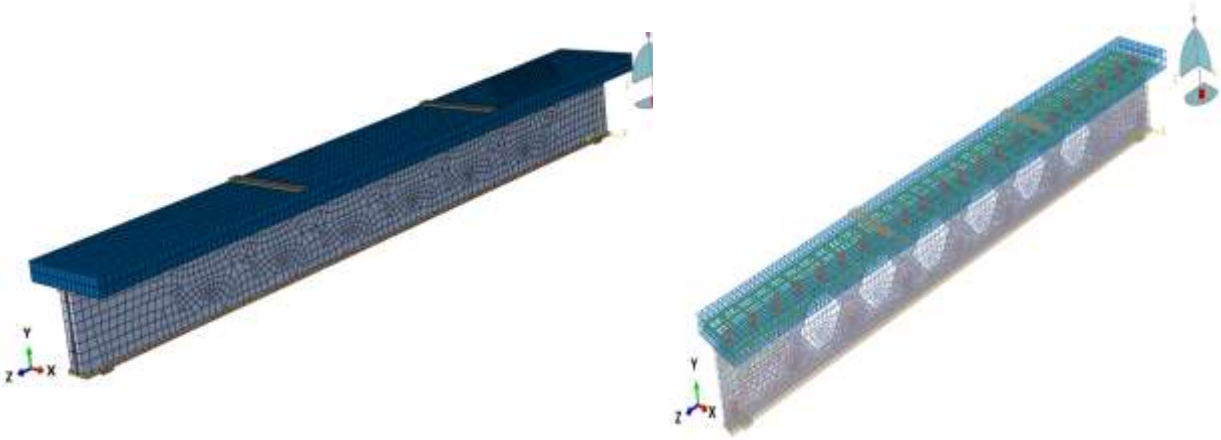

(c) No.3

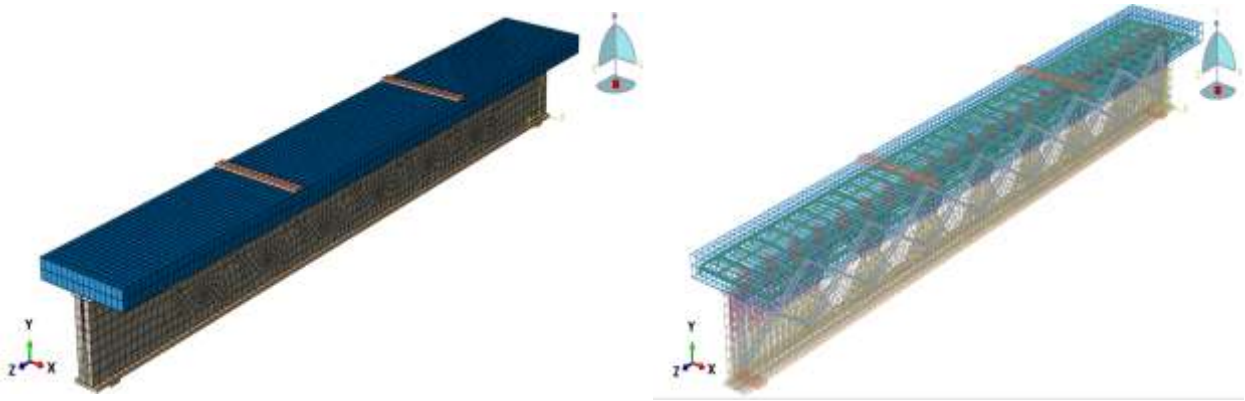

(d) No.4

Figure 11. Finite element modelling for all models.

3.2 Numerical Results and Discussion

3.2.1 Ultimate load

The ultimate load for all numerical analysis models is illustrated in **Fig. 12**. There is an increase in ultimate load compared with Ref. model No.1(S.B. without castellation and strengthening)by about (22.74%, 51.65% and 77.98%) in models(No.2, No.3 and No.4) respectively, as shown in **Table 5**.
These increased in ultimate loads back to increase in plastic sec. modulus by using the castellated operation**(Fares et al., 2016)** because of an increase in depth of the steel beam, about 52.52% compared with the Ref. model, and strengthening by R.P.C., and lacing rebars.

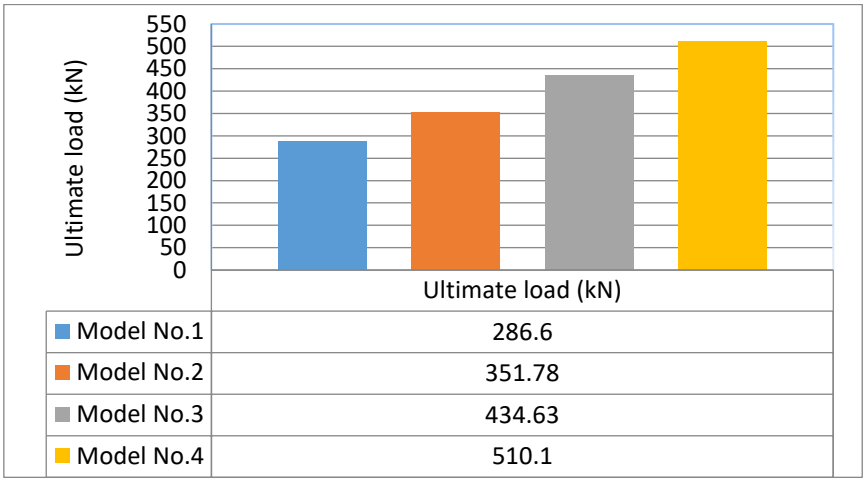

Figure 12. Ultimate load for all models.

Table 5. The difference in ultimate load for all models analysis.

Model No.	Ult. load Pu (kN)	Change in Ult. load $\frac{Pu - Pu,Ref.}{Pu,Ref.} 100(\%)$
1(Ref.)	286.6	–
2	351.78	22.74
3	434.63	51.65
4	510.1	77.98

3.2.2 Deflection and failure mode

According to the findings, the castellated process in model No.2, the castellated with strength of the R.P.C. on steel web in model No.3 and the castellated with strength of the R.P.C., and lacing in model No.4, there is a reduction in deflection about (55.52%, 58.74 and 60.55%) in models(No.2, No.3 and No.4) respectively, as shown in **Table 6**, compared to the level deflection at ultimate load for reference model No.1(blue dotted line) in **Fig. 13**. **Figs. 14** to **17** illustrate the deflection results for analysis models from the start loading up to the ultimate load, while failure modes are described in **Table 6** and shown in **Figs. 18** to **21**.

Table 6. All models differ in deflection compared to the level deflection at ultimate load for reference model analysis.

Model No.	Level defl. at ult. load of Ref. model Δ (mm)	Change in ult. Load (%) $\frac{\Delta - \Delta u, Ref.}{\Delta u, Ref.} 100$	Failure mode
1(Ref.)	16.75	–	Flexural, buckling in the top flange and yielding in the bottom flange.
2	7.45	-55.52	Flexural and yielding in the bottom flange.
3	6.91	-58.74	Flexural, local buckling in the web and shear.
4	6.55	-60.89	Flexural, yielding in the bottom flange, local buckling in a top flange, crushing in the concrete slab and shear in R.P.C.

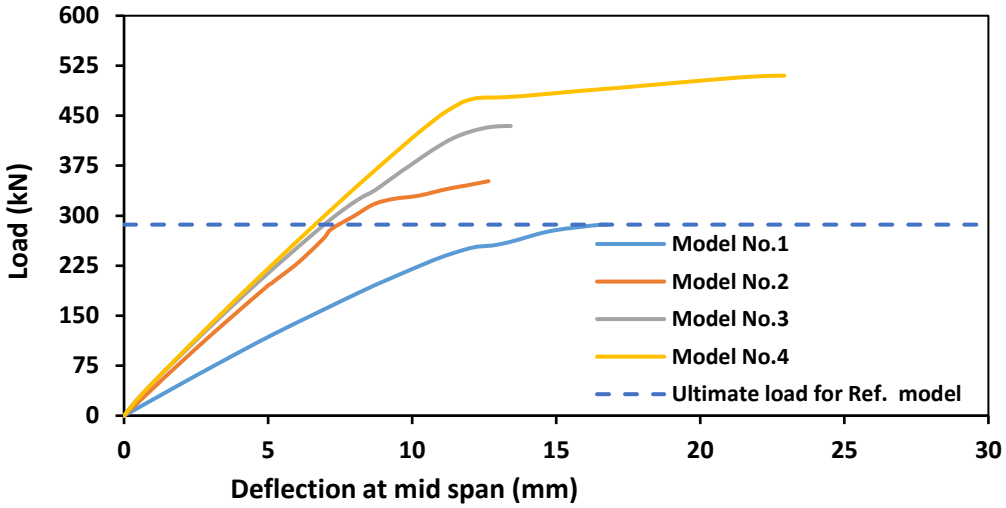

Figure 13. Load – mid-span deflection for all analysis models.

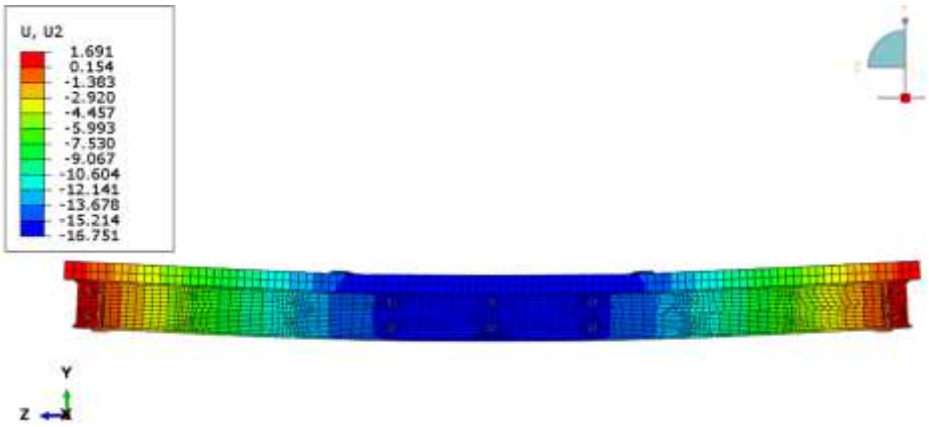

Figure 14. The values of deflections along model No.1 at the ultimate load.

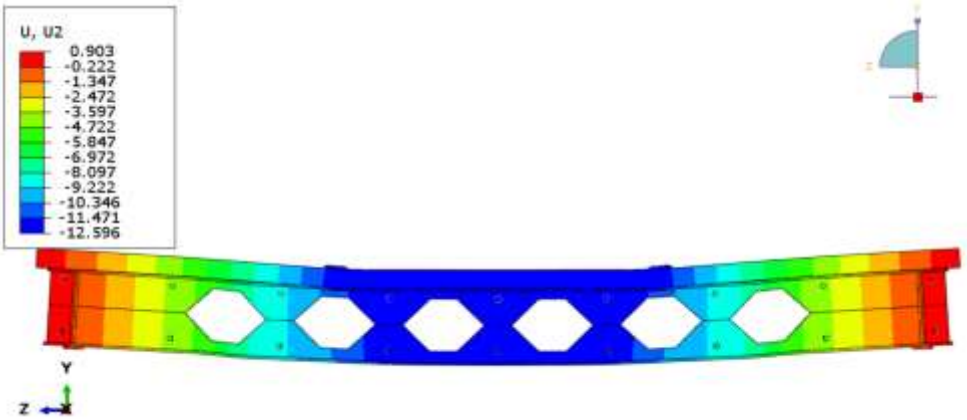

Figure 15. The values of deflections along model No.2 at the ultimate load.

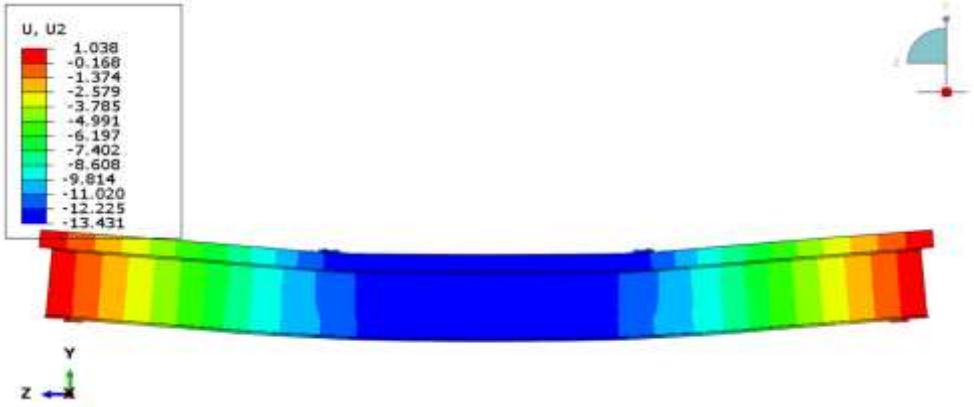

Figure 16. The values of deflections along model No.3 at the ultimate load.

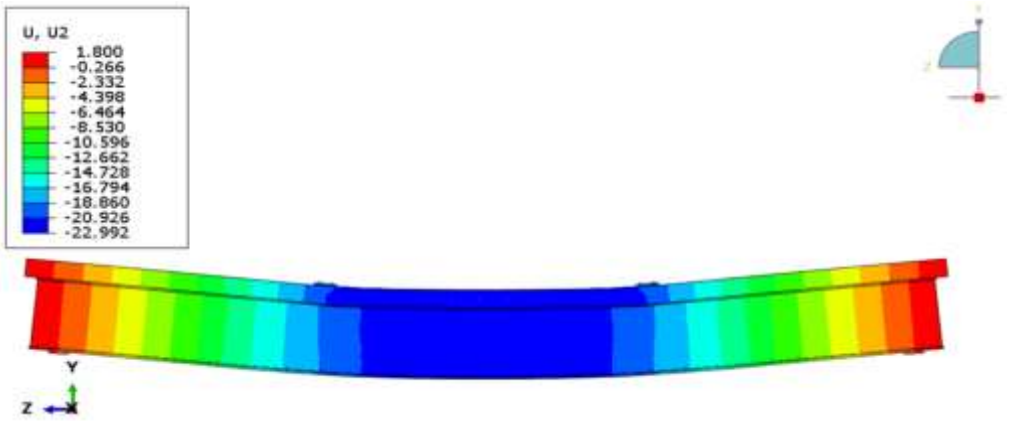

Figure 17. The values of deflections along model No.4 at the ultimate load.

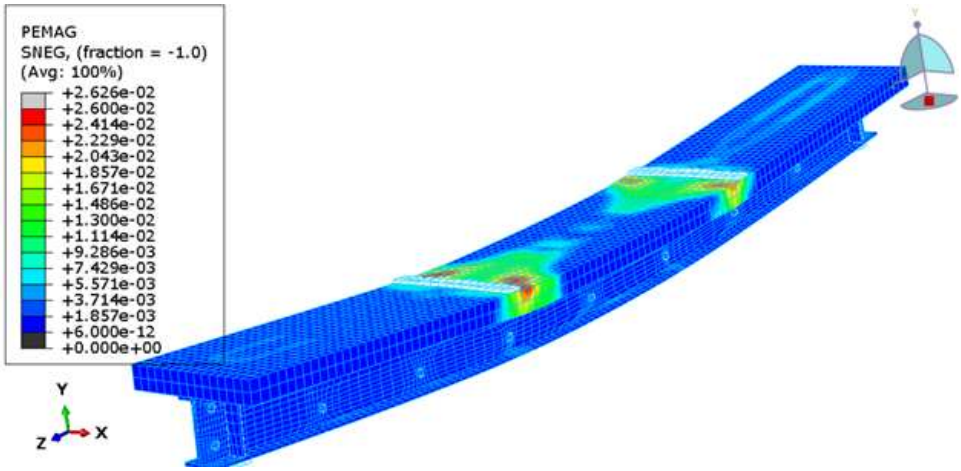

Figure 18. The failure mode of model No.1.

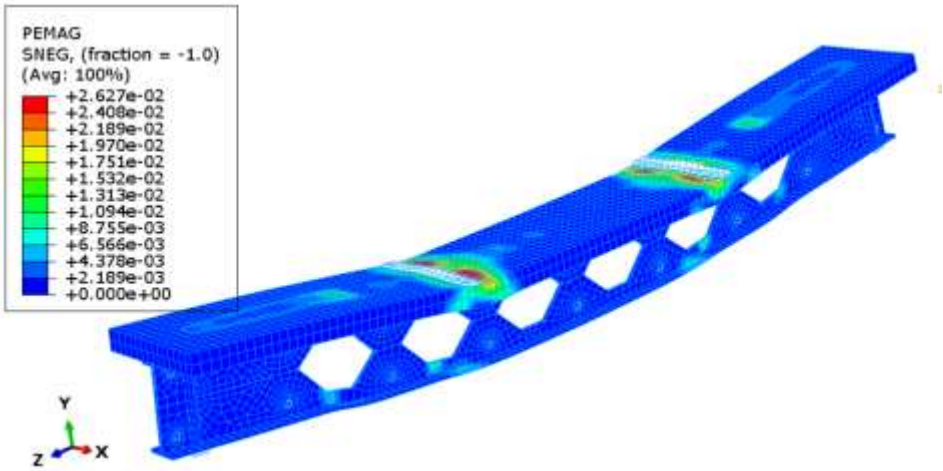

Figure 19. The failure mode of model No.2.

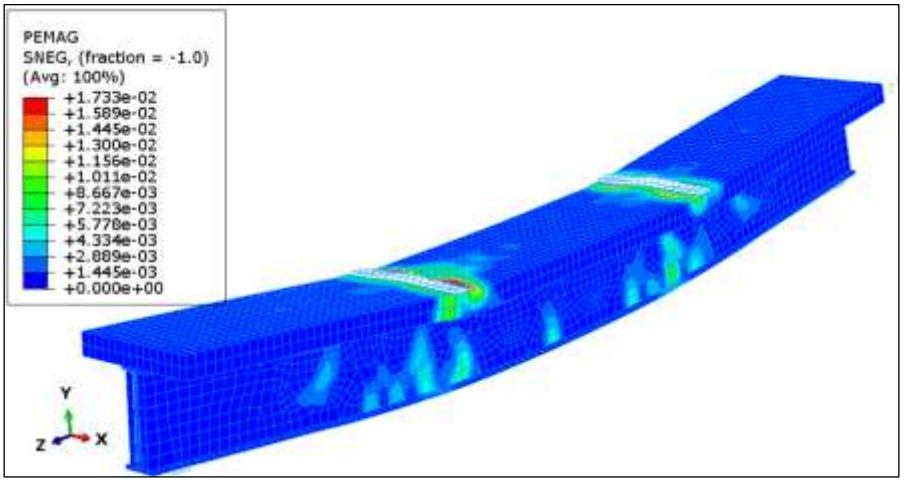

Figure 20. The failure mode of model No.3.

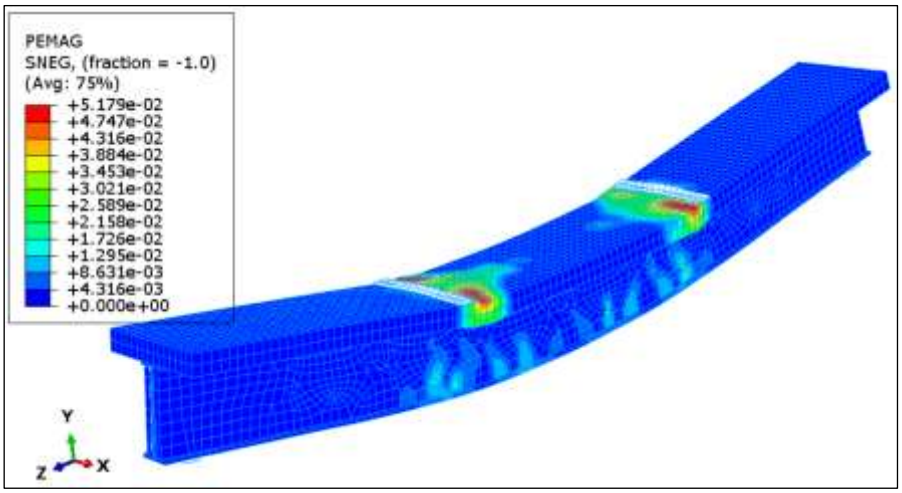

Figure 21. The failure mode of model No.4.

3.2.3 Stiffness

The load demanded as a result of unit deflection is referred to as stiffness. **(Ahmad and Abou Saleh, 2018)**. Stiffness values were derived using finite element analysis deflection and ultimate load values. All models have increased stiffness compared to Ref. model No. 1 because of increased section dimension and rigidity due to the castellation and strengthening procedure. **Table 7** and **Fig. 22** show the stiffness values.

Table 7. Stiffness values of the analysed models.

Model No.	$P_{ult.}$ (kN)	$\Delta_{Ult.}$ (mm)	Stiffness= $\frac{Pult.}{\Delta Ult.}$ (kN/mm)	Increase in stiffness %
1(Ref.)	286.6	16.75	17.11	-
2	351.78	12.65	27.80	62.47
3	434.63	13.421	32.38	89.24
4	510.1	22.97	22.20	29.74

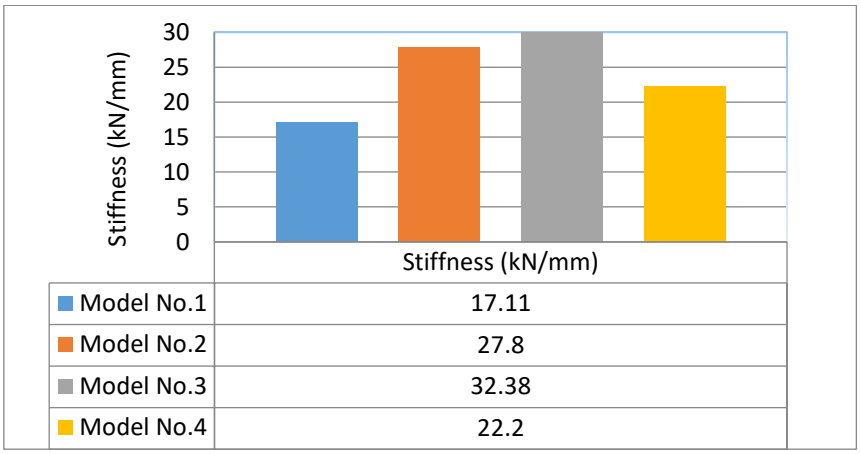

Figure 22. Stiffness values for all analysed models.

3.2.4 Ductility

The ability of a member to withstand inelastic deformations after yield deformation without observing a significant reduction in load-carrying capacity is defined as ductility. When constructing structures for various circumstances of stress, ductility is an important factor to consider. The ductility of flexural members' can be calculated using its load-deflection curves. (**Hallawi and Al-Ahmed, 2019).** The ductility factor (μ) is defined as a ratio of the failure deflection to the yield deflection, as shown in Eq. (7):

$$\mu = \Delta \mu / \Delta y \quad (7)$$

where; Δ μ is the mid-span deflection at maximum load, and Δy is the first yield mid-span deflection.

Table 8 and **Fig. 23** illustrate the ductility factor results from yield and ultimate loading stage mid-span deflection values acquired from numerical analysis. The result reveals that the factor of the ductility is raised compared to Ref. model No.1, is increased by (31.38%, 50.36% and 56.20%) in models (No.2, No.3 and No.4) respectively; this increase was related to using castellated process and strengthened with R.P.C., and rebars lacing, led to considerable increasing in flexural elements.

Table 8. The ductility factor for the analysed models.

Model No.	Δ_y (mm)	$\Delta_{ult.}$ (mm)	Ductility factor $\mu = \frac{\Delta ult.}{\Delta y}$	Increase in ductility %
1(Ref.)	12.21	16.75	1.37	-
2	7.00	12.65	1.80	31.38
3	6.50	13.421	2.06	50.36
4	10.72	22.97	2.14	56.20

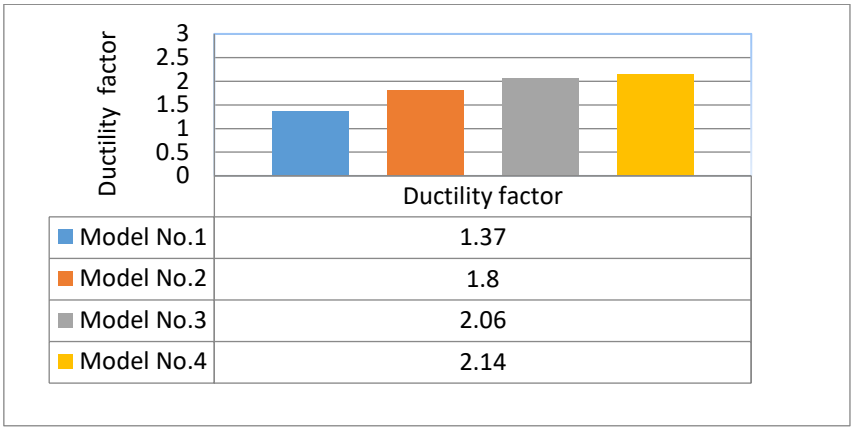

Figure 23. Ductility factor for all analysed models.

4. CONCLUSIONS

The theoretical analysis of composite concrete asymmetrical castellated hot-rolled double steel channels(2C) joined back to back by bolts, with or without strengthening techniques, under simply supported reactions with two concentrated static loads, and its results from the ABAQUS program led to the following conclusions:

- The ultimate load increased by around 22.74%, 51.65%, and 77.98% when compared to the reference model for the castellated model, castellated with R.P.C model., and castellated with R.P.C. reinforced by lacing model, respectively.
- A reduction in beam deflection at the loading level of about 55.52%, 58.74%, and 60.55% for the castellated model, castellated with R.P.C. model and castellated with R.P.C. reinforced by lacing model, respectively, when compared to the reference model.
- An increase in stiffness of about 62.47%, 89.24% and 29.74%, as, An increase in Ductility of about 31.38%, 50.36% and 56.20% for the castellated model, castellated with R.P.C. model, and castellated with R.P.C. reinforced There by lacing model, There respectively, when compared to the reference model.
- An increase in net openings spans for strengthening models compared to a standard castellated beam.
- Double steel channels are characterised by the freedom of rotation and reflection through cutting and fabricated to castellated form without losses in cutting steel at the ends of the castellated beam, unlike the castellated I section.

5. ACKNOWLEDGEMENT

The University of Baghdad/Iraq, which provided funding for this study's completion as well as assistance and support from the Civil Engineering Department, is acknowledged by the authors.

NOMENCLATURE

Symbols	Definitions	Symbols	Definitions
d_c	Scalar compression damage variable	Δ μ	Mid-span deflection at maximum load
d_t	Scalar tension damage variable	Δy	Ultimate deflection at yield load
E_0	Initial Young's modulus	$\varepsilon_c^{in,h}$	Inelastic compression strain of concrete
f_r	Modulus of rupture, in MPa	$\varepsilon_c^{pl,h}$	Plastic hardening strain in compression of concrete
f_y	Yield Strength of Steel, in MPa	Ɛcr	Cracking strain
P_u	Ultimate load to beam.	ε_{cu}	Strain of concrete corresponding in compression
$P_{u,Ref.}$	Ultimate load of reference beam	$\varepsilon^{pl}{}_{true}$	Plastic true strain
P_y	Yield load to beam	Ɛt	Nominal tension strain
t_w	Web thickness, in mm	ε_t^{ck}:	tension strain
t_f	Flange thickness, in mm	$\varepsilon_t^{pl,h}$	Plastic hardening strain in tension of concrete
Δ	Mid-span deflection, in mm	σ_c	Nominal compressive stress of concrete
Δu	Ultimate deflection at Ultimate load	σ_t	Nominal tension stress
μ	Ductility factor	σ_{true}	True stress

REFERENCES

Abdullah, Md. Sabri. 1993, Reinforced concrete beams with steel plates for shear. Ph.D. Thesis, Department of Civil Engineering. University of Dundee, UK.

ABAQUS Analysis User Guide, 2013. http://50.16.176.52/v6.13/

Ahmad, S., Masri, A., and Abou Saleh, Z., 2018. Analytical and experimental investigation on the flexural behaviour of partially encased composite beams. *Alexandria Engineering Journal*, *57*(3), pp. 1693-1712. Doi:10.1016/j.aej.2017.03.035

Al-Hilali, A.M., and Izzet, A.F., 2023. 3D-ABAQUS modelling of prestressed concrete hunched beams with multi-openings of different shapes. *Journal of Engineering*, *29*(08), pp. 149-170. Doi:10.31026/j.eng.2023.08.11

Alkloub, A., Allouzi, R., and Naghawi, H., 2019. Numerical nonlinear buckling analysis of tapered slender reinforced concrete columns. *International Journal of Civil Engineering*, *17*, pp. 1227-1240.

Al-Tameemi, S.K., and Alshimmeri, A.J., 2023, February. Behavior of asymmetrical castellated composite girders by gap in steel web. In AIP. Conference Proceedings (Vol. 2414, No. 1). AIP. Publishing. Doi:10.1063/5.0116809

Al-Thabhawee, H.W., 2017. Experimental study of effect of hexagonal holes dimensions on ultimate strength of castellated steel beam. *Kufa Journal of Engineering*, 8(1), pp. 97-107. Doi:10.30572/2018/KJE/811186.

Altifillisch, M.D., Cooke, B.R., and Toprac, A.A., 1957. An investigation of open web expanded beams. *Welding Research*, *22*(2).

American Institute of Steel Construction Inc. (AISC), Steel Construction Manual (15th Edition). 2017.

Ammar, H.A., and Alshimmeri, A.J.H., 2021. A Comparison Study between Asymmetrical Castellated Steel Beams Encased by Reactive Powder Concrete with Laced Reinforcement. Key Engineering Materials, 895, pp. 77-87. https://www.scientific.net/KEM.895.77#:~:text=https%3A//doi.org/10.4028/www.scientific.net/KEM.895.77

Bangash, M.Y. H., 1989. Concrete and concrete structures: Numerical modeling and applications, Elsevier Science Publishers Ltd., London, England, 1989.

Boyed, J. P., 1964. Castellated beam-new development. AISC National Engineering Conference, AISC Engineering Journal, 3, pp. 106-108.

British Standard Institution, BS5950, 2000. Structural use of steelwork in building. Part1. Code of Practice for Design Rolled and Welded Sections.

CAE ABAQUS. User's Manual. 2011. ABAQUS analysis user's manual.

Chaudhari, S.V., and Chakrabarti, M.A., 2012. Modeling of concrete for nonlinear analysis using finite element code ABAQUS. *International Journal of Computer Applications*, 44(7), pp. 14-18.

Collins, M.P., Mitchell, D., and Macgregor, J.G., 1993. Structural design considerations for high strength concrete. *Concrete International*, 15(5), pp. 27–34.

Dakhel, Z.H., and Mohammed, S.D., 2022. Castellated beams with fiber-reinforced lightweight concrete deck slab as a modified choice for composite steel-concrete beams affected by Harmonic load. *Engineering, Technology & Applied Science Research*, 12(4), pp. 8809-8816.

Das, P.K., 1984. Handbook for the design of castellated beams (Vol. 10). Taylor & Francis.

Demir, A., Ozturk, H., and Dok, G., 2016. 3D Numerical modeling of RC deep beam behavior by nonlinear finite element analysis. *Disaster Science and Engineering*, 2(1), pp. 13-18

Ellobody, E., 2014. Design examples of steel and steel-concrete composite bridges. *Finite Element Analysis and Design of Steel and Steel-Concrete Composite Bridges*, pp. 221-467.

Fares, S., Coulson, J., and Dinehart, D., 2016. Castellated and cellular beam design. *American Institute of Steel Construction*.

Hadeed, S.M., and Alshimmeri, A.J.H., 2019. Comparative study of structural behaviour for rolled and castellated steel beams with different strengthening techniques. Civil Engineering Journal, 5(6), pp. 1384-1394. Doi:10.28991/cej-2019-03091339

Hafezolghorani, M., Hejazi, F., Vaghei, R., Jaafar, M.S.B., and Karimzade, K., 2017. Simplified damage plasticity model for concrete. *Structural engineering international*, *27*(1), pp. 68-78. Doi:10.2749/101686616X1081

Hallawi, A.F., and Al-Ahmed, A.H.A., 2019. Enhancing the behavior of one-way reinforced concrete slabs by using laced reinforcement. *Civil Engineering Journal*, *5*(3), pp. 718-728. Doi:10.28991/cej-2019-03091282

Khaleel, A.I., and AL-Shamaa, M.F., 2021. Experimental Investigation on the Structural Behavior of Double Channel Castellated Steel Beams. In *E3S Web of Conferences* (Vol.318,p.03009).EDPSciences. Doi:10.1051/e3sconf/202131803009

Knowles, P.R., and BS 5950, 1991. CASTELLATED BEAMS. Proceedings of the Institution of Civil Engineers, 90(3), pp. 521-536.

Lee, J., and Fenves, G.L., 1998. Plastic-damage model for cyclic loading of concrete structures. *Journal of Engineering Mechanics*, *124*(8), pp. 892-900.

Lubliner, J., Oliver, J., Oller, S., and Onate, E., 1989. A plastic-damage model for concrete. *International Journal of Solids and Structures*, *25*(3), pp. 299-326.

Matthews, F.L., Davies, G.A.O., Hitchings, D., and Soutis, C., 2000. Finite element modelling of composite materials and structures. Woodhead Publishing Limited, Abington Hall, Abington Cambridge CB1 6AH, England

Mohammed, H.H., and Ali, A.S., 2023. Flexural behavior of reinforced rubberized reactive powder concrete beams under repeated loads. *Journal of Engineering*, *29*(8), pp. 27-46. Doi:10.31026/j.eng.2023.08.03

Oukaili, N.K., and Al-Shammari, A.H., 2014. Finite element analysis of reinforced concrete T-beams with multiple web openings under impact loading. *Journal of Engineering*, *20*(06), pp. 15-27. Doi:10.31026/j.eng.2014.06.02

Qasim, O.A., 2019, May. Comparative study between the cost of normal concrete and reactive powder concrete. In *I.O.P. Conference Series: Materials Science and Engineering* (Vol. 518, No. 2, p. 022082). I.O.P. Publishing. Doi:10.1088/1757-899X/518/2/022082

Reddiar, M.K.M., 2010. *Stress-strain model of unconfined and confined concrete and stress-block parameters*. (Doctoral dissertation, Texas A & M University).

Toprac, A.A., and Cooke, B.R., 1959. *An experimental investigation of open-web beams*. Welding Research Council.

Waryosh, W.A., and Ali, A.S., 2020. Effects of web opening size on the behavior of castellated concrete geopolymer composite beam. *International Journal of Latest Engineering Research and Applications (IJLERA),* 5(5) pp. 17-28. Doi:10.31272/jeasd.conf.1.39